spin Orbit torque memory for cache & multicore processor applications

www.spot-research.eu

D3.2: 1st compact model of the magnetic device

Responsible CNRS Spintec (G. Di Pendina)

Dissemination Level Public (PU)

Date of preparation: October 25th, 2013

Particip.	Participant organization name	Short name	Country
1 RES 1	CNRS Spintec	CNRS	France
2 RES 2	Catalan Institute of Nanotechnology	ICN	Spain
3 RES 3	Karlsruher Institut für Technologie	KIT	Germany
4 RES 4	National Center for Scientific Research Demokritos	NCSR D	Greece
5 RES 5	CEA LETI	LETI	France
6 IND 1	In Silicio	INSIL	France
7 IND 2	Singulus	SING	Germany
8 OTHER 1	Toplink Innovation	TLI	France
9 RES 6	Eidgenössische Technische Hochschule Zürich	ETHZ	Switzerland
No.	**Advisory Board member**	**Short name**	**Country**
TAB 1	Micron Technology	MICRON	Italy
TAB 2	Tower Semiconductor	TOWER	Israel
TAB 3	European Nanoelectronics Infr. for Innovation	ENI2	Europe

Work programme topics addressed

Objective ICT-2011.3.1: Very advanced nanoelectronic components: design, engineering, technology and manufacturability

a) "Beyond CMOS technology"

Name of the coordinating person: Gilles Gaudin

e-mail: gilles.gaudin@cea.fr **Tel:** +33 (0)4 38 78 23 84

Table of contents

1st compact model of the magnetic device – Work Package 3 "Standard Cell Modeling and Design"

1. INTRODUCTION

The WP3 includes 2 different aspects of the design environment included in Task 3.2:
First of all the Process Design Kit (PDK), which is related to the process. The PDK enables to draw and check the layout of all the masks of the demonstrator to be fabricated, including CMOS and magnetic steps. Since up to now the CMOS and the post-process foundries have not been clearly identified, nothing has been done yet. Indeed it is absolutely dependent on the process and on the CAD tool environment.
Second of all, the PDK includes electrical simulations based on device compact models. Concerning the CMOS devices, it is also dependent on the CMOS process, however, concerning the Spin Orbit Torque magnetic device it is not related to the CMOS process but only to the magnetic post-process. Thus, the requested work for the D3.2 deliverable has been done and validated. This is described in detail belowis to develop a compact model in order to be able to run electrical simulations for ASIC design.

2. SPIN ORBIT TORQUE DEVICE AS IMPLEMENTED IN THE COMPACT MODEL

The development of the SOT device compact model is based on the nano-fabrication scheme illustrated on *Figure 1*, provided by WP2 partners.

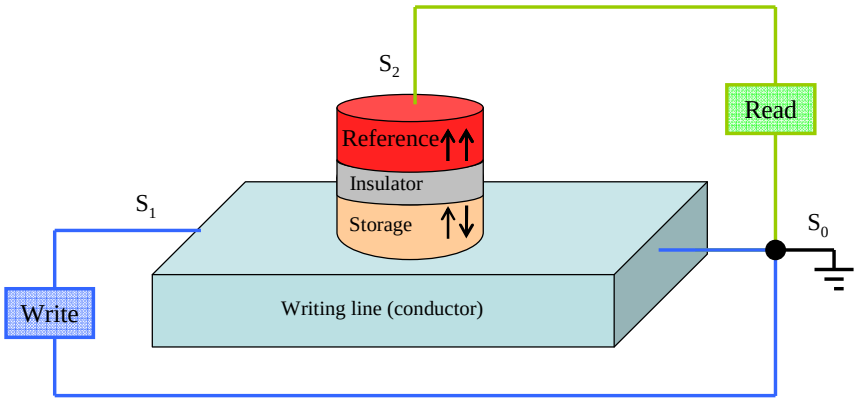

Figure 1: Schematic of the three-terminal SOT device and the two independent paths for read and write operations. In-plane current injection through the write line (conductor) induces the perpendicular switching of the storage layer.

To reverse the magnetization of the storage layer, in-plane current pulses are injected through the conductor. Depending on the sign of injected current (positive or negative), bipolar reversal magnetization of the storage layer is achieved (up or down). Here, we stress on the necessity of an external static magnetic field of moderate amplitude, also commonly called bias field. This external applied field is required to coexist with Rashba and Spin Hall effects in order to achieve the magnetic reversal of the storage layer in one direction or another when applying a pulse of courant. It is a static magnetic field. Neither its value nor its exact orientation is critical for the reversal. This field H_a contributes to the control of switching when a pulse of writing current is applied. Without this bias field the storage layer switching would be random, depending on the moment the injected current is stopped during the damping phase of the storage layer switching. *Figure 2* illustrates the theoretical behavior of the SOT-MTJ in the presence of a permanent magnetic field: Starting from the initial magnetization, the AP or the P states are obtained by applying a negative current pulse or a positive current pulse, respectively. In *Figure 2*, the permanent magnetic field is negative (B_a<0). It is also possible to work with a positive B_a (B_a>0). The effect of the current pulses will be simply inverted, as explained in the pseudo code in *Figure 2c*. Finally, *Figure 2d* gives the chronograms of the SOT device behavior.

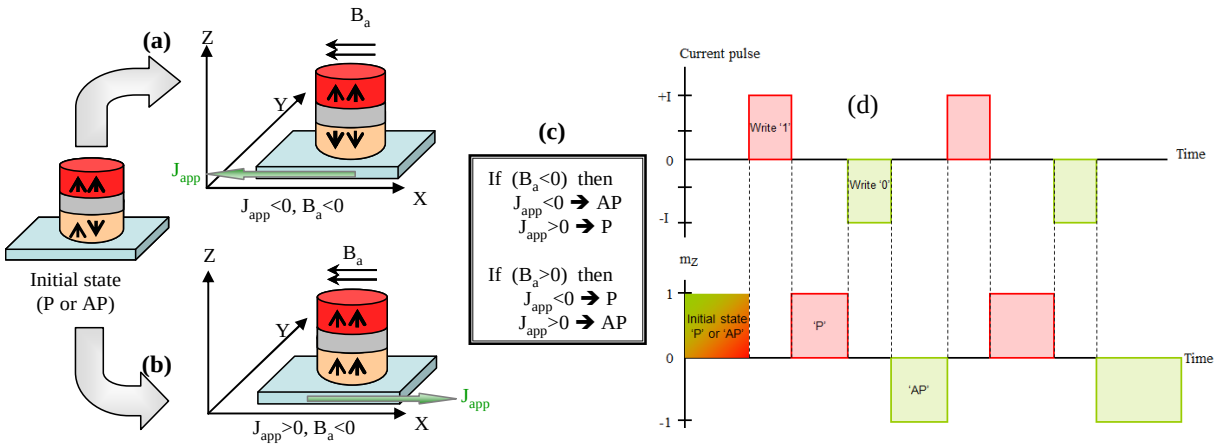

Figure 2: Switching dependence on the applied field and current directions

2.1 COMPACT MODELING OF THE SOT DEVICE

In this work, we provide the first compact model written in Verilog-A of a SOT-MTJ. Our choice of the coding language is motivated by the capability of Verilog-A to afford a quick method of enhancing compact models to illustrate new physics of advanced processes. In addition, it is on the path to becoming the preferred compact modeling language for both academic and industrial research groups thanks to its flexibility to run in numerous simulators (Spectre, HSpice, ADS, Eldo…) and internal simulators of semiconductor companies. First,

we analyze the model equations along with some approximations. Then, thanks to close interactions with Spintec technologists, a number of associated parameters are fed into these equations. The simulator translates the established equations as equivalent circuit elements.

2.1.1 SOT-MTJ modeling strategy

The SOT-MTJ model describes the dynamic magnetic behavior of the single domain storage layer as a function of the current density injected through the conductor underneath it.

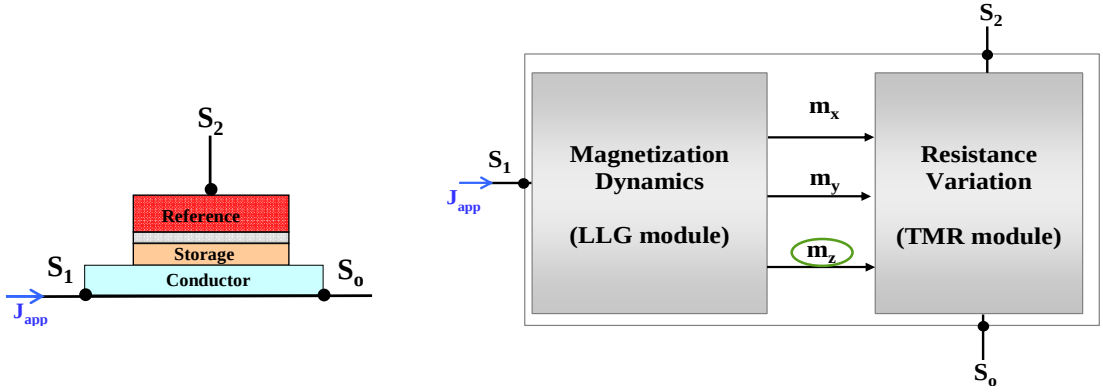

(a) Physical view of the SOT-MTJ *(b) Block diagram of the compact model*

Figure 3: Modeling strategy of the three-terminal SOT-MTJ

The physical model of the SOT MRAM cell in *Figure 3(a)* illustrates the layers and the signal interface for its input and output signals. *Figure 3(b)* gives a block diagram showing the whole SOT-MTJ module connections. As shown, there are 3 external nodes: S_1 and S_0 are used for the writing path, S_1 and S_0 are used for the reading path. Also, 3 internal connections m_x, m_y and m_z which represent the three components of the storage layer magnetization represented as voltages are represented. The whole block diagram is composed of 2 main modules: the LLG module and the TMR module.

2.1.2 LLG module

The LLG module describes the dynamic evolution of the storage layer magnetization as a function of time and applied current density (J_{app}). This module has one input (J_{app}) which represents the current applied through the write line (S_1S_0) of the device to control the magnetization reversal of the storage layer. The 3 outputs m_x, m_y and m_z represent the magnetization components in a Cartesian system.

This module implements the Landau–Lifshitz–Gilbert equations:

$$\frac{\partial \vec{m}}{\partial t} = -\frac{\gamma_0}{1+\alpha^2}(\vec{m}\times\vec{H}_{eff}) - \alpha\frac{\gamma_0}{1+\alpha^2}\vec{m}\times(\vec{m}\times\vec{H}_{eff}) \quad (1)$$

Where $\vec{m}$ is the unit vector along the magnetizations of the soft layer, α is the Gilbert damping constant, γ_0 is the gyromagnetic ratio and $\vec{H}_{eff}$. The first term in equation (1) describes the precession of the magnetization around the effective magnetic field. The second term in equation (1) is the Gilbert damping torque which forces the magnetization to relax towards the effective field. The effective field is the sum of the different magnetic fields which acts on the storage layer magnetization:

$$\vec{H}_{eff} = \vec{H}_k + \vec{H}_d + \vec{H}_R + \vec{H}_{SHE} + \vec{H}_a$$

with the magneto crystalline anisotropy field (H_k), the demagnetizing field (H_d), the Rashba field (H_R), the SHE field (H_{SHE}) and the external applied field H_a

The interaction between the magnetic moment and the crystalline lattice is responsible for a privileged direction that we will denote as $\vec{z}$, in which the magnetization will spontaneously align itself without external field. The equivalent magneto crystalline anisotropy field is expressed as:

$$\vec{H}_k = \frac{2K_u}{\mu_0 M_s} m_z \vec{z} \quad (2),$$

with K_u is the uniaxial anisotropy constant, and M_s is the spontaneous magnetization value.

Another source of anisotropy is the shape of magnetic nanostructures via the magneto static energy. The magnetization always tends to align with the longest dimension of the ellipsoid in magnetic ellipsoidal nanostructures. This effect is described in the model using the following equation:

$$\vec{H}_d = -M_s \begin{bmatrix} n_x & 0 & 0 \\ 0 & n_y & 0 \\ 0 & 0 & n_z \end{bmatrix} \begin{bmatrix} m_x \\ m_y \\ m_z \end{bmatrix} \quad (3)$$

with n_x, n_y and n_z are demagnetizing tensor coefficients

The Rashba effect field and the Spin Hall Effect (SHE) field are the two original components of the total effective field $\vec{H}_{eff}$ which differ the SOT-MTJ from other MTJ generations (FIMS, TAS, and STT). Their key role in the magnetic switching of ferromagnetic dots has given the birth to a new concept of three-terminal MRAM that we are describing in this work. Based on the experiments and the interpretations afforded by SPINTEC technologists, the Rashba effect and the SHE fields are expressed according to the following equations, respectively:

$$\vec{H}_R = C_R J_{app} \vec{y} \quad (4)$$

$$H_{SHE} = -C_{SHE} J_{app} \vec{m} \times \vec{y} \quad (5)$$

C_R is the Rashba coefficient, C_{SHE} is the SHE coefficient and J_{app} is the density of current applied in the conductor.
$\vec{H}_a$ is the external magnetic field necessary to ensure deterministic magnetic reversal storage layer. In our model, we admit that the external applied field is expressed as: $\vec{H}_a = H_a \vec{x}$ (6).

2.1.3 TMR module

The second module of the Verilog-A model is the TMR module which describes the magneto resistance variation based on the orientation of the storage and reference layers (P/AP). It takes the output of the LLG module as its inputs and it depends basically on the m_x and m_z component of the magnetization as shown below in equation.
Following the first TMR model by Jullière and Slonczewski's further work, the tunneling conductance is a function of the angle between the magnetizations of the two FM layers. Furthermore, the bias-dependent conductance of the device at 0K can be derived in the framework of Brinkman's model and Simmons's model. By combining formulas given by these complementary models, we can assume that the total tunneling conductance can be expressed according to the equation (25):

$$g(V, m_x, m_z) = \frac{G_{P0}(1 - 2\beta V + 3\delta V^2)}{1 + \left(\frac{1 - (m_x \cos\theta_{mhl} + m_z \sin\theta_{mhl})}{2}\right)\left(\frac{tmr_0}{1 + \frac{V^2}{V^2{}_h}}\right)} \quad (7)$$

Where β and δ are tunnel oxide material-dependent constants, G_{P0} is the conductance in parallel magnetic configuration at 0V and 0K usually calculated from Simmons's model. V represents the bias voltage applied across the device and tmr_0 is the tunnel magneto resistance under a low bias voltage. V_h is defined as the voltage at which the TMR amplitude has decreased to half of its low bias value ($tmr(V_h)=tmr_0/2$). θ_{mhl} corresponds to the magnetic state of the hard layer (reference layer).

2.2 ELECTRICAL SIMULATION ENVIRONMENT USING THE COMPACT MODEL

In this section, we present simulation results for the MTJ cell run with Spectre simulator under Cadence Virtuoso platform. We also investigate the impact of the current density, the pulse width and the external applied field on the behavior of the MTJ dynamics. We note that the following conventions are used in the discussion of simulation results: i) the initial magnetization state of the SOT-MTJ is in the parallel state (P) .i.e. the magnetization of the reference layer and the storage layer are along the z-axis with upward orientation (at initial

state, we have the perpendicular magnetization along z-axis thus m_z=1). ii) The initial external applied field H_a has a negative value. iii) Negative current pulse switches the MTJ configuration into the AP state while positive pulses switch the MTJ configuration into the P state in the presence of a negative H_a.

A set of experimental-based parameters from is fed into the model for simulations, among which the geometrical parameters such as the shape, the size, the initial magnetic state of the MTJ and the other physical and technological parameters. The current density threshold required for switching the magnetization from P (AP) to AP (P) has the same value (symmetrical switching). It is of the order of $J_{app} = 10^{12}A.m^{-2}$. We admit that the SHE factor (C_{SHE}) is twice the value of Rashba coefficient (C_R). All this parameters can be easily tuned by the user as current experimental work proceeds. *Figure 4* gives the schematic used for the electrical simulation under Cadence / Schematic Composer environment. A single SOT device is connected to current and voltage sources. This enables both writing and reading phases.

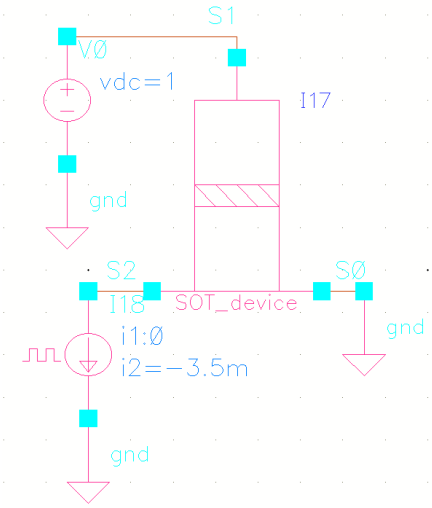

Figure 4 : Schematic of the SOT device characterization

2.2.1 Impact of current density and pulse width on the perpendicular magnetization m_z

We study in *Figure 5* the dynamic evolution of the m_z component for different values of applied current density (J_{app}) based on the experimental results published for this type of device which claim that J_{app} must be in the order of $10^{12}A.m^{-2}$.

We choose to begin our study with a negative pulse of 3ns and vary the current density value to observe the dynamics of switching. *Figure 5(a)* shows that at $J_{app} = -1x10^{12}A.m^{-2}$, the spin torque is not enough to act on the magnetization of the storage layer, the initial state (m_z=1) is retained during and after the pulse. Starting from a value of $J_{app} = -2x10^{12}A.m^{-2}$, we can notice the manifestation of a spin torque action on the magnetization. But, because of the shortness of the applied pulse, it was not possible to attain the reversal of the magnetization.

If we apply a larger pulse, the magnetization occurs. This is confirmed in *Figure 5(b)* where we vary the pulse width with a fixed current density of $J_{app} = -2x10^{12}A.m^{-2}$. So, when we apply large pulses, a lower current is required for switching. From *Figure 8(a)*, we notice that the higher is the value of J_{app}, the smaller is the width of the pulse required for switching. For example, at $J_{app}= 4x10^{12}A.m^{-2}$, the width of the pulse could be only 0.3 ns instead of the 3ns applied and could decrease further (~ 0.1ns for $J_{app}= 8x10^{12}A.m^{-2}$).

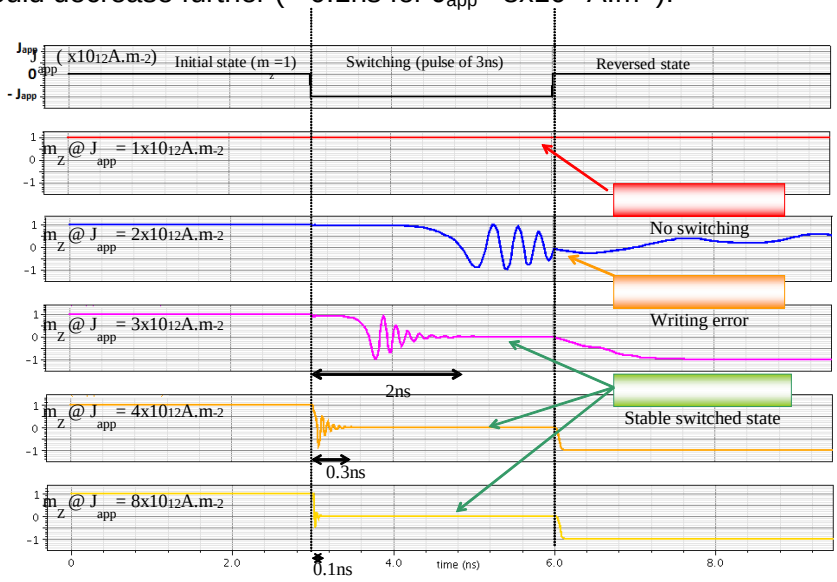

(a) Evolution of m_z according to the current density J_{app}

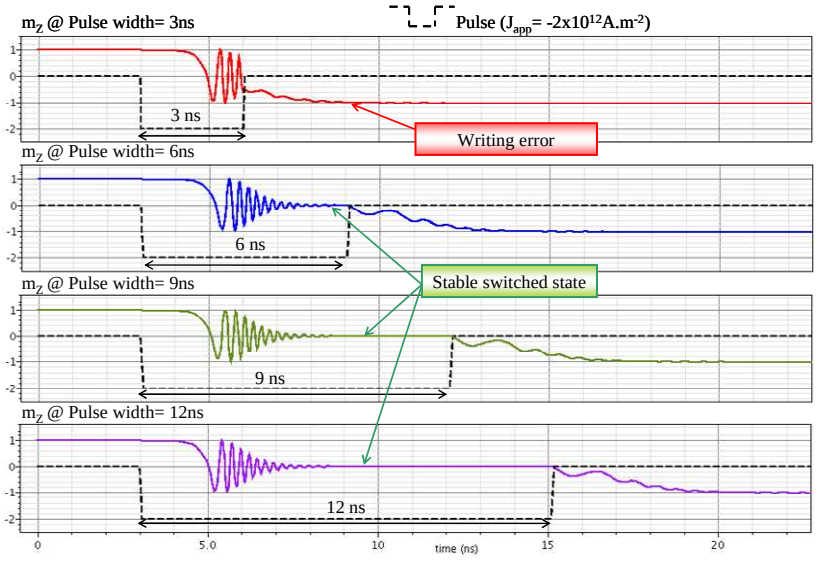

(b) *Evolution of m_z according to the pulse width @ $J_{app} = -2x10^{12}$ A.m^{-2}*

Figure 5: Study of the dynamic behavior of the perpendicular magnetization m_z according to the variation of the current density J_{app} and the pulse width

To sum up, based on the simulations results, at least a current density of $2x10^{12}A.m^{-2}$ is required to make the magnetization reversal occur at large pulses (~6ns). For higher current density the required pulse width decreases further to attain hundreds of picoseconds starting from a current density of $4x10^{12}A.m^{-2}$. These simulation results show a good agreement with experimental measurement where the magnetization switching is achieved at J_{app}~ $2x10^{12}A.m^{-2}$ with a pulse width of 9ns.

2.2.2 Impact of the external field H_a on the magnetization reversal

Figure 6(b) illustrates the random switching obtained, as the theoretical predictions, in the absence of an external magnetic field. In our case, the reversal in one direction or another, when H_a=0, is probably due to numerical noise. The solution used by research teams working on the realization of the SOT device, is the generation of a permanent magnetic field H_a by adding a permanent magnet on chip or a biasing layer on top of MTJs.

Figure 6(a) shows a proper reversal of the magnetization m_z according to the current pulse in the presence of a negative bias field. If a negative pulse is applied, the magnetization is reversed downward (m_z=-1) while a positive pulse switches the magnetization upward (m_z=1). *Figure 6(c)* shows that the response to the current direction can also be inverted by reversing the direction of Ha (reversing the polarization of the magnets responsible for the generation of the static magnetic field H_a). Finally, we verified the fact that we do not require high values of applied field to reverse the magnetization as shown in *Figure 6(d)*, where we used 3 different values of H_a and observed that the value of applied field is not crucial in the reversal mechanism, a small value is sufficient.

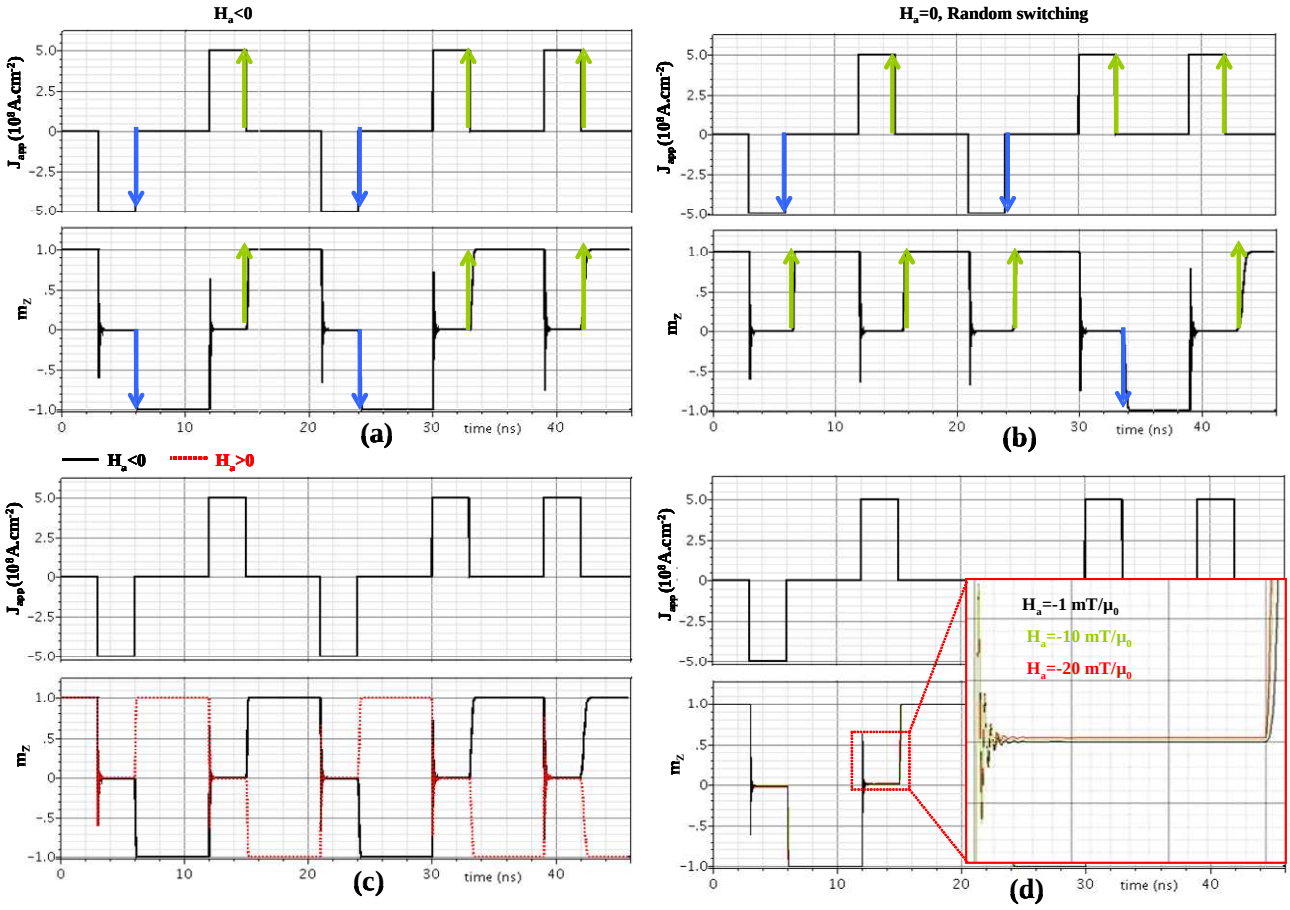

Figure 6 : Study of the dynamic behavior of the perpendicular magnetization m_z according to the variation of the sign and value of the external applied field H_a

2.2.3 Magneto resistance variation as a function of the applied current

Figure 7 a) and b) shows the simulation results of m_z reversal according to the current pulse in the presence of a negative field (B_a<0). If a negative pulse on J_{app} is applied, the magnetization is reversed downward (m_z=-1) while a positive pulse on J_{app} switches the magnetization upward (m_z=1). In our model, the influence of this external field has been implemented giving the completed behavior of the SOT device.

In *Figure 7 b) and c)*, we investigate the variation of the SOT-MTJ magnetization as a function of the current through the MTJ during a reading phase. We fixed the bias voltage at 1V and we observed the evolution of the current for both cases parallel and anti-parallel. For the parallel state P (m_z=1), we notice a higher current value of 8.75µA (i.e. lower resistance) and for the state AP (m_z=-1), we notice a lower current value of 7.3µA (i.e. higher resistance). Thus, the model describes correctly the dependence of the MTJ resistance on the state of the perpendicular magnetization m_z which in turn depends on pulses of the writing current.

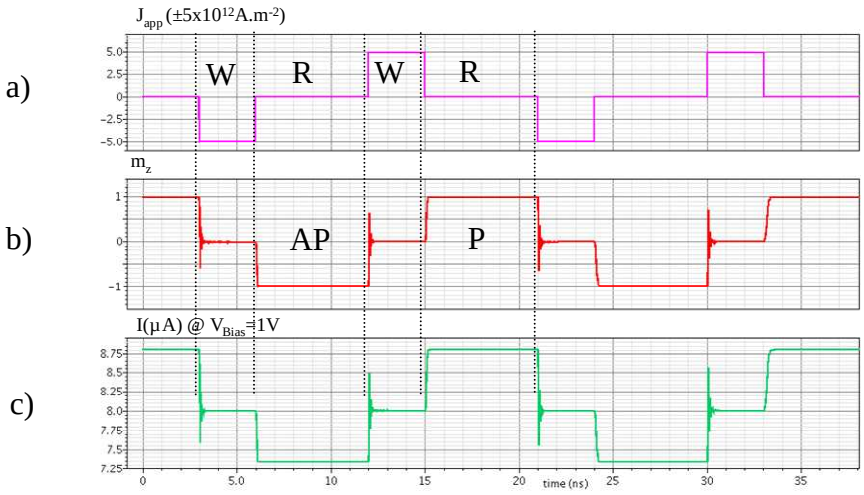

Figure 7 : Validation of the magneto resistance variation according to current pulses or MTJ states

3. CONCLUSION

The WP3 of SPOT project includes mainly 3 tasks. One of them, Task 3.2 is supposed to last 24 months, from T0 to T0+24. A full compact model has been developed and validated and the deliverable D3.2 has been provided to all the partners on time, at TO+12 as scheduled. This model is customizable and will be adapted to the magnetic process as the features will be more and more accurate. The Process Design Kit will be developed as soon as both CMOS and magnetic foundries will be chosen and will integrate this compact model. Then, the Design Rule Manual (DRM) will be provided as well. Therefore, the design of specific hybrid standard cell architectures will be now possible using this compact model.